

**Detection of Freezing of Gait
in Patients with Parkinson's Disease
using Electroencephalography
and Computational Intelligence**

By

Aluysius Maria Ardi Handojoseno

A thesis submitted in partial fulfilment of the requirements for the degree of
Doctor of Philosophy



Faculty of Engineering and Information Technology

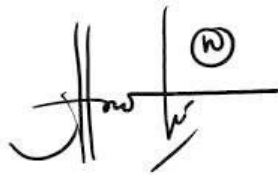
2015

Certificate of Authorship/Originality

I, Aluysius Maria Ardi Handojoseno, certify that the work in this thesis has not previously been submitted for a degree, nor has it been submitted as part of the requirements of a degree, except as fully acknowledged within the text.

I also certify that this thesis has been written by me. Any help that I have received in my research work and in the preparation of the thesis itself has been acknowledged. In addition, I certify that all information sources and literature used are indicated in the thesis.

Signature of Candidate:

A handwritten signature in black ink, consisting of stylized cursive letters and a horizontal line, with a small circled 'w' or similar mark to the right.

Date: 26 November 2015

“Teach us to give and not to count the cost”

St. Ignatius Loyola

Acknowledgements

First and foremost, I thank God, whose many blessings have made me who I am today, and enabled me to complete the research.

I would like to express my heartfelt appreciation and sincere gratitude to my principal supervisor, Professor Hung Tan Nguyen, Professor and Director, Centre for Health Technologies, University of Technology, Sydney, for the opportunity to carry out this research and for his invaluable guidance throughout. His experience and expertise in Health Technologies provided crucial insights for the research presented in this work.

I would also like to express my thanks to Dr Yvonne Tran and Dr Tuan Nghia Nguyen, my co-supervisors. Their guidance and support were exceptional. Their advice always enlightened and encouraged.

My sincere gratitude also goes to Dr Simon J.G. Lewis, Dr James 'Mac' Shine, and Moran Gilat at the Parkinson's Disease Research Clinic, Brain and Mind Research Institute, University of Sydney, for their collaboration in collecting data, analyzing results, and writing papers for journals and conferences. I hope we can further our collaboration on new projects in the near future.

My special thanks to all my colleagues and staff members at the Centre for Health Technology, University of Technology, Sydney, especially Dr. Mitchell Yuwono for his compelling enthusiasm and support, and to Quynh Tran Ly who will continue to work on this project.

Finally and importantly, my deep appreciation goes to the Indonesian and Australian Jesuits for the mission and all support of doing this research, my Jesuit community in St. Mary's North Sydney especially to Father Daven Day, and to my Indonesian Jesuit friends, and to Mum and my family, for their constant love, understanding, encouragement, moral support and prayer throughout. And special thanks also to my friends especially Reena Maria Francesca Tolmik, Penny Ho, Gracelyn Vega, Gems Surya and family, Fenty Terihardjo and Bernadette Soesanto.

Contents

List of Figures	ii
List of Tables	viii
Nomenclature	x
Abstract	xii
1 Introduction	1
1.1 Motivation	1
1.2 Problem Statement	5
1.3 Thesis Objective	7
1.4 Thesis Contribution	8
1.5 Outline of Thesis	9
1.6 Publications	10
2 Literature Review	13
2.1 Parkinson's Disease	13
2.2 Freezing of Gait	19

2.2.1	Gait Disturbance and Freezing of Gait in PD	19
2.2.2	Treatment of FOG	27
2.3	Current Strategies of FOG Detection	28
2.3.1	The Beginning of the FOG Detection Research: the Search for the Indicators of FOG	30
2.3.2	Unfreeze Attempt and Online Detection of FOG	32
2.3.3	Machine Learning in FOG Detection	35
2.4	Discussion and the Proposed Strategy for FOG Detection	38
3	EEG-Based Detection of FOG Using Artificial Neural Networks	41
3.1	Introduction	41
3.2	System Overview	42
3.3	Data Acquisition	43
3.3.1	Participants	43
3.3.2	Procedure	43
3.3.3	Signal Preprocessing	47
3.4	Feature Extraction	47
3.4.1	Power Spectral Density	49
3.4.2	Centroid Frequency	51
3.4.3	Power Spectral Entropy	51
3.4.4	Wavelet Energy	52
3.4.5	Centroid Scale	56
3.4.6	Wavelet Energy Entropy	56

3.5	Feature Selection	57
3.6	Artificial Neural Networks Classification Algorithm	58
3.6.1	Architecture	59
3.6.2	Learning of Artificial Neural Networks	60
3.7	Experimental Results	64
3.8	Discussion and Conclusion	73
4	Detection of FOG Using Brain Signal Spectral Coherence	76
4.1	Introduction	77
4.1.1	Limitations of Segregated Spectral Analysis in EEG-Based FOG Detection	77
4.1.2	Advantages of Functional Integration Features	77
4.2	System Overview	81
4.3	Synchronization of the Cortical Activity Measurements	81
4.3.1	Magnitude-Squared Coherence	81
4.3.2	Wavelet Coherence	85
4.3.3	Weighted Phase Lag Index	86
4.3.4	Phase-Locking Value	88
4.4	Feature Selection and Artificial Neural Networks Classification	89
4.5	Experimental Results	90
4.6	Discussion and Conclusion	99
5	Advanced FOG Detection Using ICA and Brain Effective Connectivity	101
5.1	Introduction	102

5.2	System Overview	105
5.3	Data Preprocessing: Maximization of Non-Gaussianity of the EEG Feature Set Using FastICA	107
5.4	Causality Measures of Brain Signals for Detecting FOG Episodes	109
5.4.1	Multivariate Autoregressive Process	110
5.4.2	Squared Generalized Partial Directed Coherence	111
5.5	Feature Selection and Artificial Neural Networks Classification	116
5.5.1	Improving the Generalization Using Bayesian Regularization	117
5.6	Experimental Results	118
5.7	Discussion and Conclusion	129
6	Discussion and Future Work	132
6.1	Discussion	132
6.2	Conclusion	136
6.3	Future Directions	137
	Appendix A Research Ethics Clearance	139
	Appendix B Publications	142
	Bibliography	197

List of Figures

1.1	Projected growth rates in number of individuals over 50 with PD in the most populous nations in Western Europe and the world from 2005 to 2030	3
2.1	Dopamine roles in the movement production as a neurotransmitter.	14
2.2	Comparison of control movement between healthy state and PD	15
2.3	Schematic diagram of the nervous system for normal movement	15
2.4	Schematic diagram of converging sensory flow to the inferior-posterior parietal lobule (Joseph, 1996).	16
2.5	Schematic diagram of the motor control flow (Carlson, 2013).	17
2.6	Main functional division of the cortico-basal connections (Juri <i>et al.</i> , 2010).	18
2.7	Clinical impact of FOG (Okuma, 2014).	20
2.8	Imagery-related brain activity in right superior parietal area.	21
2.9	Imagery-related brain activity in the left supplementary motor area.	24
2.10	Imagery-related brain activity during motor imagery of gait along a narrow path (Bakker <i>et al.</i> , 2008).	25
2.11	Sample averaged MRP with two prominent peaks	25
2.12	Three-dimensional stereotactic surface projection image	26
2.13	Treatment of FOG (Okuma, 2014).	27

2.14	Frequency characteristics of normal (near 2 Hz) and FOG (6-8 Hz) of the 3 dimensional acceleration measurement (x: horizontal, Y: vertical, z: transverse)	30
2.15	The freeze index (FI=red trace) was calculated from the power in the freeze band (38 Hz) divided by power in the locomotor band (0.53 Hz). Large peaks occurred during FOG (Moore <i>et al.</i> , 2008).	31
2.16	Laser Cane, a walking stick with a bright red line laser beam projection to help the PD patient overcome freezing episodes (Constantinescu <i>et al.</i> , 2007).	33
2.17	The GaitAid Virtual Walker visual cueing device transmits image of tiled floor to a projector fitted to glasses. The tiles image moves in response to the patient's movements, prompting the brain to keep the leg muscles going. Earphones provide additional help to improve walking, by giving auditory feedback	34
2.18	FOG detection and feedback device developed by Bächlin <i>et al.</i> (2009) with sensors attached to the shank, the thigh and the lower back	35
2.19	Sensitivity and specificity plots for the Bachlin <i>et al.</i> (2010)'s online detection device accuracy using (a) global parameter (b) subject-dependent parameter	36
2.20	The GaitAssist system for a PD patient daily-life assistant with inertial measurement unit sensors (1), 2 functionalities for training support and FOG detection (2 and 3), preferences setting (4), audio feedback (5) and logging module (6)	37
3.1	Signal processing flows for detecting FOG from the EEG data	42
3.2	Location of four electrodes related to cortical control of movement	45

3.3	(A) The timed up and go (TUG) task for FOG assessment. (B) Four different trials with different additional tasks to trigger a freezing condition during walking from a chair to a taped box on the floor and back to chair (Shine <i>et al.</i> , 2012).	46
3.4	The sample of EEG signal before and after the band-pass and the band-stop filtering during freezing episodes in the time domain	48
3.5	Frequency distribution of the EEG signal before and after filtering stage .	48
3.6	The EEG signal is divided into 8 segments with a 50 % overlap between each segment in the Welch method of spectral analysis. The output is the averaged data of the 8 transforms which are calculated separately.	50
3.7	Sample PSD from subject 7 channel P4; the mean of the PSD indicates the significant increase of power during transition to FOG in alpha and beta frequencies	51
3.8	Multi-Resolution Analysis	54
3.9	Decomposition of EEG into detail (d1-d5) signals related to five standard clinical EEG subbands by db4 wavelet taken from electrode P4 in subject 6 shows the amplitude and frequency alterations preceding and during freezing episode.	55
3.10	Biological neuron (Carlson, 2013).	58
3.11	Perceptron, a model of a neuron.	59
3.12	Feedforward networks with 1 hidden layer and 1 output layer.	60
3.13	A summary flow graphs of back-propagation learning with the forward pass on the top part of the graph and backward pass on the bottom part of the graph	61
3.14	Shift of CF in electrode Cz in 3 mid-range frequencies band. Decreasing of centroid frequency in beta frequency band of normal walking signifies transition to freezing episode.	67

3.15	Shift of CS in electrode Fz in 3 mid-range frequency bands. Decreasing of centroid frequency in theta frequency band of normal walking signifies freezing episodes.	67
3.16	Boxplot of PSE of 3 different conditions and 4 EEG electrodes in beta frequency band.	68
3.17	Boxplot of WEE of 3 different conditions and 4 EEG electrodes in beta frequency band.	68
3.18	Testing result of using CF at centroid zero as input for the MLP-NN with different number of hidden nodes.	69
4.1	Brodman area functional atlas.	78
4.2	Publications search rates recorded by PubMed.gov. U.S. National Library of Medicine shows an increase in the number of studies looking for information on functional segregation (activation) and functional integration (connectivity)	79
4.3	System overview of FOG detection using functional integration features of EEG data	80
4.4	Subject 1 - samples extracted from electrodes P4 and O1 of cross power spectral density and magnitude-squared coherence under 3 conditions. . .	83
4.5	Wavelet cross spectrum for transition of freezing at gamma sub-band. The upper panels shows EEG signals from electrode pairs O1 and P4. The right panel presents the global wavelet spectrum obtained by averaging over time samples.	87
4.6	Boxplot of MSC of EEG signals during normal walking and transition to FOG (frequency band 5, used electrode 4) with number 1, 2, 3, 4, 5 and 6 in the x-axes referring to O1-P4, O1-Cz, O1-Fz, P4-Cz, P4-Fz and Cz-Fz respectively. The asterisk indicates p -value <0.05 . A higher number of the asterisk refers to a higher r -value.	92

4.7	Boxplot of wavelet coherence of EEG signals during normal walking and transition to freezing of gait (frequency band 5, used electrode 4) with number 1, 2, 3, 4, 5 and 6 in x-axes refer to O1-P4, O1-Cz, O1-Fz, P4-Cz, P4-Fz and Cz-Fz respectively. The asterisk indicates p -value <0.05 . A higher number of the asterisk refers to a higher r -value.	93
4.8	Phase synchronization measured using the WPLI.	95
4.9	Phase synchronization measured using the PLV.	95
5.1	False flow (dotted arrows) of signal from B to C can be found as the result of the different delays (Δ_1 and Δ_2) of the propagation of signals (blue arrow) from A to B and A to C	105
5.2	2 different patterns of connectivity amongst 3 channels. In the left networks, there is a direct pathway from A to C, while in the right networks there is 1 indirect pathway from A to C only	105
5.3	System overview for detecting FOG from the EEG data using BEC features	106
5.4	Mixing and blind separation of the EEG signals using ICA	107
5.5	sGPDC Flowchart	114
5.6	sGPDC functions calculated for experimental data and surrogate data of subject 7. The results of surrogate data show the “leak flows” between channels, which determine the thresholds for considering the significant flows.	115
5.7	Optimal model order selection using SBC on the study data sample of transition condition in subject 1. The minimum value, 6, is the optimal model order.	118
5.8	Information flow between locations of interest during normal walking and transition to FOG, estimated with the sGPDC function for 0.5-60 Hz frequency band in patient 8. The arrow width in the diagram (right column) depicts the connectivity strength between locations of interest.	121

5.9	Causality values in the theta frequency bands of the overall population of subjects extracted using dDTF. The asterisk symbol indicates significant difference between normal waking and transition to freezing in the locations pair (p -value <0.05 ; r -value >0.2).	122
5.10	Causality values in the theta frequency bands of the overall population of subjects extracted using sGPDC. The asterisk symbol indicates significant difference between normal waking and transition to freezing in the locations pair (p -value <0.05 ; r -value >0.2).	123
5.11	The schematic alteration interaction between 4 locations of EEG electrodes during normal walking and transition to FOG estimated using (A) dDTF and (B) sGPDC at theta band frequency. The solid line arrow represents the significant increase in connectivity strength and the dash line arrow indicates the significant decrease in connectivity strength.	123
5.12	Comparison of the levels of separation of BEC features extracted from EEG data during normal walking and transition to FOG using dDTF (top row) and sGPDC (bottom row), without ICA (left column) and with ICA (right column) measured with Pearson's correlation coefficient r	125
5.13	Graphical depiction of the predicted mechanism underlying FOG	131

List of Tables

1.1	The Hoehn & Yahr Scale (1967)	4
2.1	Studies on pathophysiology of FOG	22
2.2	Overview of selected studies of lower gait movement, FOG, and related brain location	23
2.3	Studies on the detection of FOG	29
3.1	Patient's demographics, neurological, cognitive and freezing characteristics	44
3.2	Frequency bands corresponding to different decomposition levels	54
3.3	Correlation analysis of normalized PSD and normalized WE between normal walking (N), transition to FOG (T), and FOG (F). The result of the statistical analysis shows the separability of EEG signals using power based features.	65
3.4	Classification results of proposed Fourier Transform based features using MLP-NN in detecting transition 5 s before freezing from normal walking.	71
3.5	Classification results of proposed Wavelet Transform based features using MLP-NN in detecting transition 5 s before freezing from normal walking.	72
4.1	Correlation analysis of CPSD and WCS between normal walking (N), transition to FOG (T), and FOG (F) in 3 mid-range frequency bands	91

4.2	Classification results of proposed Fourier transform based features using MLP-NN to detect the 5 s transition before freezing from normal walking	96
4.3	Classification results of proposed wavelet transform based features using MLP-NN to detect the 5 s transition before freezing from normal walking	97
4.4	Features Rank based on the average of the classification accuracy	98
4.5	Classification results of combination features using MLP-NN in detecting transition 5 s before freezing from normal walking	98
5.1	Correlation analysis of effective connectivity in 0.5-60 Hz frequency band between normal walking, transition to FOG, and FOG estimated by dDTF and sGPDC	119
5.2	Correlation analysis of Effective Connectivity in the 0.5-60 Hz frequency band between normal walking, transition to FOG, and FOG estimated using dDTF and sGPDC with ICA	124
5.3	Comparison between classification performance of the neural network structure of 1 to 20 hidden nodes with input sGPDC+ICA+BR	126
5.4	Classification results of the neural network with BEC as feature, using early stopping in training, to detect the 5 s transition before freezing in normal walking	127
5.5	Classification results of the neural network using BEC as the features, optimized by using Bayesian regularization in training or ICA data pre-processing	128
5.6	Classification results of the neural network using BEC as the features, optimized by using Bayesian regularization in training and ICA data pre-processing at a time.	129
6.1	Best performance of proposed methods in detecting transition 5 s before freezing from normal walking	134

Nomenclature

3D-SSP	:	3-dimensional Stereotactic Surface Projections
AD	:	Alzheimer Disease
ANN	:	Artificial Neural Networks
APSD	:	Auto-Power Spectral Densities
AR	:	Autoregressive
BA	:	Brodmann Area
BSS	:	Blind Source Separation
CPSD	:	Cross Power Spectral Density
CS	:	Centroid Scale
CWT	:	Continuous Wavelet Transform
DALY	:	Disability Adjusted Life Years
dDTF	:	Direct Directed Transfer Function
DNN	:	Dynamic Neural Network
DSM-IV	:	Diagnostic and Statistical Manual of Mental Disorder, Fourth Edition
DTF	:	Directed Transfer Function
DWT	:	Discrete Wavelet Transforms
EEG	:	Electroencephalography
EMG	:	Electromyography
EOG	:	Electrooculography
ffDTF	:	Full Frequency Directed Transfer Function
FFT	:	Fast Fourier Transform
FI	:	Freeze Index
fMRI	:	Function Magnetic Resonance Imaging
FOG	:	Freezing of Gait
FOG-Q	:	Freezing of Gait Questionnaire
H&Y	:	Hoehn and Yahr

ICA	: Independent Component Analysis
MEG	: Magnetoencephalography
MGAP	: Microbe Genome Annotation Platform
MLP-NN	: Multi Layer Perceptron Neural Networks
MMSE	: Mini Mental State Examination
MRP	: Movement-Related potentials
MSC	: Magnitude Squared Coherence
MVAR	: Multivariate Autoregressive
NFOG-Q	: New Freezing of Gait Questionnaire
PCA	: Principle Components Analysis
Pcc	: Pearson's Correlation Coefficient
PD	: Parkinson's Disease
PDC	: Partial Directed Coherence
PLV	: Phase Locking Value
PSD	: Power Spectral Density
PSE	: Power Spectral Entropy
PWF	: Patient with PD with FOG
PWoF	: Patient with PD without FOG
PWP	: Patient with PD
RAS	: Rhythmic Auditory Stimulation
ROI	: Region of Interest
RT	: Reaction Time
SCF	: Spectral Centroid Frequency
sGPDC	: Squared Generalized Partial Directed Coherence
SMA	: Supplementary Motor Area
SPECT	: Single Photon Emission Computed Tomography
TUG	: Timed Up and Go
UPDRS	: Unified Parkinson's Disease Rating Scale
VBM	: Voxel-Based Morphometry
WCO	: Wavelet Coherence
WCS	: Wavelet Cross Spectrum
WE	: Wavelet Energy
WEE	: Wavelet Energy Entropy
WPLI	: Weighted Phase Lag Index
WPS	: Wavelet Power Spectrum

Abstract

Freezing of Gait (FOG) is a common movement disorder affecting patients with Parkinson's disease in the advanced stage. Patients often describe it as feeling like their feet are "glued to the floor" which suppresses their ability to start walking or to continue moving forward. It significantly affects patients' quality of life since the sudden and unpredictable characteristic of FOG is a common cause of falls and related injuries. It interferes with daily activities, and leads to a loss of independence. Freezing of gait is mainly perceived as an alteration in the pattern of movement, and the accelerometer, which senses movement, speed and direction, can be used as the main sensor in the detection of FOG in research studies.

Although the accelerometer has been successfully applied in the detection of FOG, it is only able to detect FOG as it occurs, which is often too late for prevention of injuries such as falls. The research in this thesis introduces electroencephalography (EEG) as a novel technique to address this problem. The EEG provides a window to see the transition episode *before* a freezing episode. Freezing of gait occurs as a result of complex, dynamic neurophysiology in the brain related to motor control as well as cognition and emotions, and the EEG signal can capture the electrical activity of the brain while this is occurring. In addition, scalp EEG has many other benefits, such as its portability, non-invasive nature, relative inexpensive cost and simple operation, whilst providing high precision in time measurements.

The study examined 16 patients (age 70.88 ± 6.92 years) with idiopathic Parkinson's disease and significant FOG, consisted of 9 patients at Hoehn and Yahr (H&Y) stages 2 and 2.5 - the early stages (56.25%), 5 patients at stage 3 - the moderate stage (31.25%), and

2 patients at stage 4 - the advanced stage (12.5%). This research studied the various features of EEG which can be used as indicators of FOG and aims to introduce the effective features as inputs for the FOG.

The first analysis was based on the classical power spectral density (extracted using Fast Fourier Transform) and its counterpart (extracted using wavelet transform). By using centroid frequency extracted from channel central zero (Cz) as input and artificial neural network as the classifier, the classification of two episodes (normal walking and 5 s transition before freezing) in the in-group was obtained with a sensitivity, specificity and accuracy of 77.0%, 74.1% and 79.5%, respectively.

The second analysis studied the cross correlation and coherence based features, aiming to improve the performance of the FOG detection and to obtain a better understanding of FOG. These features provide spatial properties of EEG which complement the time-frequency characterization gained from classical power spectral analysis.

Beyond correlation of two brain locations, in the third analysis, the brain connectivity dynamic analysis was explored further using the analysis of the causal influence between the brain locations of interest. A squared Generalized Partial Directed Coherence was used to evaluate this causal connectivity. This approach modelled effectively the inherently multivariate nature of neuronal networks. All the features were investigated with clinical EEG data. After the optimization using Independent Component Analysis and Bayesian regularization, and applying squared Generalized Partial Directed Coherence connectivity estimation, in the in-group the classifier achieved a sensitivity, specificity and accuracy of 89.1%, 91.2%, and 90.2% , respectively. The results in the out-group were relatively similar with a sensitivity, specificity and accuracy of 86.5%, 92.8% and 89.5%, respectively.

In addition, the physiology analysis provided the characterization of FOG. Beta oscillations in central lead were found to underlie the neural activity in transition to the freezing episode in power spectral measurement. In coherence study, pairwise frontocentral showed significant change, especially in the theta frequency. Effective connectivity also showed significant alteration on the causality measurement in this area. This finding lead

to the development of the predicted mechanism underlying FOG.

In summary, the techniques proposed in this dissertation contribute to the development of the detection system of FOG that can be used by patients with PD to improve their symptoms with satisfactory classification performance. In addition, the results of the experiment provide the electrophysiological signature of FOG in PD lead to novel insights into the pattern of spatiotemporal dynamic of the brain underlying this debilitating symptom of PD.